

Average Model of a High Frequency DC-DC Converter for Fuel Cell Application in Electrical Vehicle

M. Amari⁽¹⁾, J.Ghouili⁽²⁾ and F. Bacha⁽³⁾

^{1,3}Unité de Recherche en Automatique et en Informatique Industrielle (URAI), Université de Tunis
Mansour.amari@gmail.com, Faouzi.Bacha@esstt.rnu.tn

²University of Moncton, Canada, jamel.ghouili@umoncton.ca

Abstract

In this paper a high frequency DC-DC converter fed by fuel cell is analyzed. The converter consists of full bridge inverter connected to full bridge rectifier through two planar transformers and parallel resonant. The mathematical model of the fuel cell is first presented and the average model of the converter is elaborated. The developed model is used to study the characteristics and dynamics of the DC-DC converter in closed loop. Validation of the proposed model is verified through simulation.

Keywords: Fuel cell, high frequency, planar transformer, average model, parallel resonant, DC-DC converter

I-INTRODUCTION

The reduction of gases emitted by the thermal vehicles is justifiable reason to motivate many researchers to investigate alternatives to conventional internal combustion engine.

among these studies, the development of hybrid electric vehicles that use clean and renewable energy sources as fuel cells[1]-[2]-[3].

Fuel cell is electrochemical energy conversion device which directly produce electricity, water and heat by processing hydrogen and oxygen[4]. Generally DC voltage generated by a fuel cell stack varies widely and is low in magnitude; it is between 20V and 50V at full-load, a DC-DC converter is responsible for absorbing power from the fuel cell, and therefore should be designed to match fuel cell ripple current specifications and should not conduct any negative current.[5]

Several DC-DC converters, such as push-pull, half bridge and full-bridge converters can be used to boost the low voltage of the fuel cell to the required level. The mathematical models of these converters are very important for engineers to study the system dynamic behavior. However, the power converter models are normally time varying due to the switching action [6]

Many papers are published in this field. [7] Proposes an approach for fuel cell DC-DC converter controller using dynamic evolution control. Several approaches are applied to analyze the converters as The average models and small signals

.Dynamic performance of PWM dc-dc converter has been analyzed using state space averaging method and small signals[8]. Averaged Model of a high power Dual-Phase Boost DC-DC Converter for Fuel Cell Power Supply[9].

In reference [10], the authors study the average circuit model of non-ideal basic converter operating in discontinuous conduction mode. Reference [11] studied the control method of boost and buck converter for the ultra-capacitor-fuel cell hybrid stationary power applications using small signal ac equivalent circuit model. Based on the above issues, this paper proposes an average model for fuel cell DC-DC converter which can regulate the output voltage of the converters to avoid rapid load voltage variations. The paper is organized as: The section II discusses a model of fuel cell. The section III details the topology and the operation mode. In section IX, the average model of DC-DC converter is presented. Section X evaluates the performance of small signal model and the controller design. And finally the conclusion is presented in section XI.

II-FUEL CELL MODEL

The fuel cell directly converts chemical energy into electrical energy. It reacted hydrogen and oxygen to produce electricity, water and heat, according to the following overall chemical reaction. $2H_2 + O_2 \rightarrow H_2O + Electricity + Heat$ (1)

The following figure illustrates the principle of operation of a fuel cell.

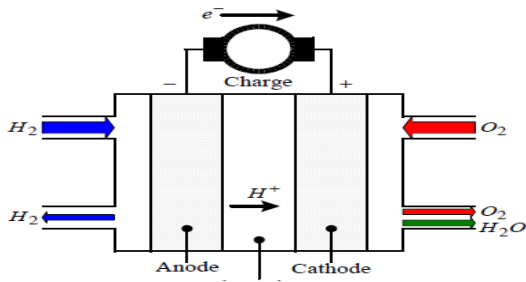


Figure 1: Illustration of a typical Fuel Cell structure

The equation of voltage fuel cell is the following:

$$V_{Cell} = E_{Nerst} - \Delta V_{act} - \Delta V_{Conc} - \Delta V_{ohmic} \quad (2)$$

Where: E_{Nerst} is the Nernst potential, ΔV_{act} is the activation loss, ΔV_{ohm} is the ohmic loss and $\Delta V_{Concentration}$ is the concentration loss. Expression of different voltages are:

$$E_{Nerst} = 1.229 + \frac{RT}{nF} \ln\left(\frac{P_{H_2} \sqrt{P_{O_2}}}{P_{H_2O}}\right) \quad (3)$$

$$\Delta V_{act} = \frac{RT}{nF} \ln\left(\frac{i}{i_0}\right) \quad (4)$$

$$\Delta V_{con} = -\frac{RT}{\alpha nF} \ln\left(1 - \frac{i}{i_L}\right) \quad (5)$$

Where P_{H_2} , P_{O_2} and P_{H_2O} are the hydrogen, oxygen and vapor partial pressures (atm), respectively. Moreover, T , is the cell temperature (K), R is the universal gas constant (8.31441 J mol⁻¹ K⁻¹), F is the Faraday constant (96484.56 C mol⁻¹), n is the number of electrons participating in the reaction, i_L is the limiting current density, i_0 is the exchange current density and α is the electron transfer coefficient of the reaction. V_{FC} is the fuel cell voltage, it can be written as follow: $V_{FC} = NV_{Cell}$ Where N is the number of fuel cell in a stack. The equivalent electrical circuit of a fuel cell is as follows:

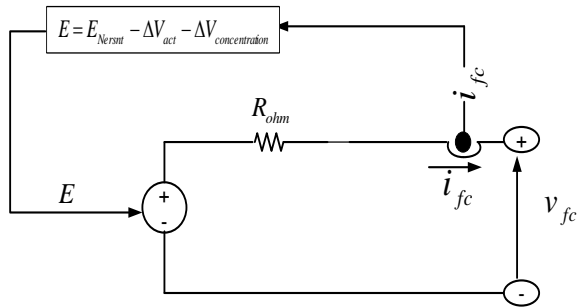


Figure 2: Fuel Cell model

Parameters of the used fuel cell are shown in the following table:

Parameter Name	Parameter Value
Temperature T	328 °K
Partial pressure of Hydrogen P_{H_2}	1.5 atm
Partial Pressure of oxygen P_{O_2}	1 atm
Partial pressure of water P_{H_2O}	1atm
Exchange current i_0	0.002A
Cell area A	0.0825m ²
Limiting current i_L	100A

Table 1:Fuel cell parameters

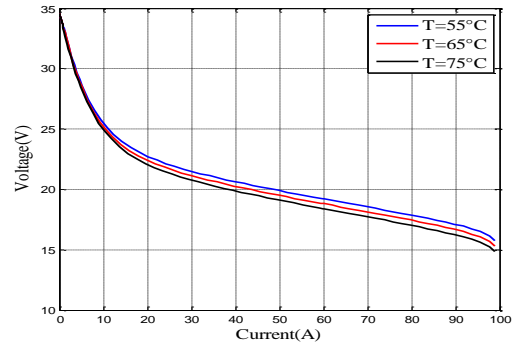


Figure 3: Fuel cell voltage versus current in various temperatures

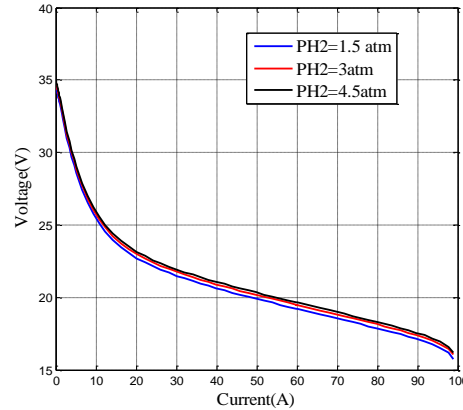


Figure 4: Fuel cell voltage versus current in various pressures

III-TOPOLOGY AND OPERATION OF CONVERTER

a) Chosen Topology

Basically, DC-DC converters can be divided into two categories depending on using the galvanic insulation or not: non-isolated converter or isolated converter [12]. as the non isolated converters are simple, but they require a bulky input inductor to limit the current ripple in the components. But, in many cases, isolation between the input and the output is required, because of operating specifications or for security reasons. It is for this reason, the use of the isolated DC-DC converters. The chosen topology is divided in three parts: a high frequency DC-AC converter, a high-frequency transformer and an AC-DC converter as shown in Figure 5.

The converter is consists of :

- Full bridge side fuel cell, it is constituted for bidirectional switches ((T_{11}, D_{11}), (T_{12}, D_{12}), (T_{13}, D_{13}) and (T_{14}, D_{14})).
- Full bridge side high voltage, it is constituted for unidirectional switches D_1, D_2, D_3 and D_4 .
- The resonant filter consists of capacitor (C_r) and inductance (L_r). its role is to minimize switching losses.
- Two planar transformers in high frequency, plays a important role in this Topology. It provides both galvanic isolation and energy storage through winding leakage inductance. The primary is coupled in parallel and the secondary are in series.

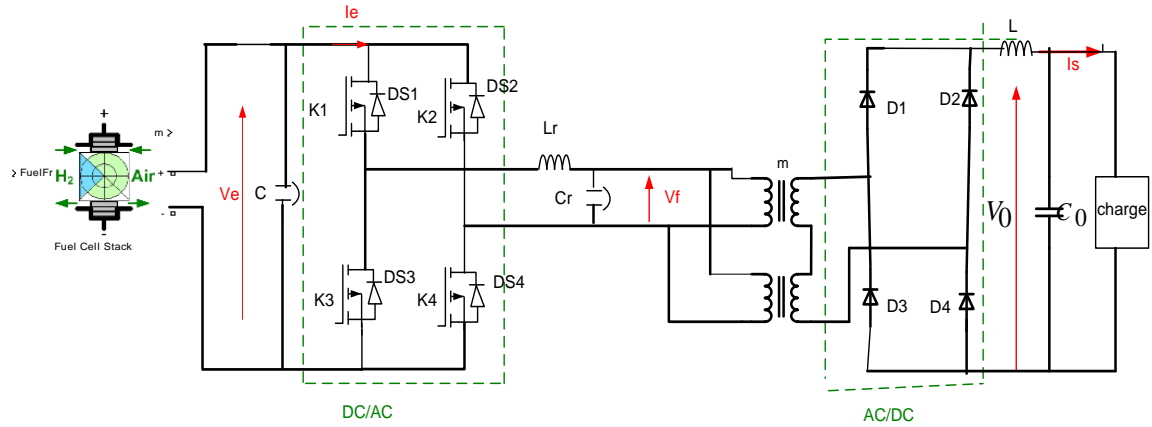


Figure 5. Topology of converter

b) Operation converter

The bridge side fuel cell is controlled to generate a high frequency wave voltage at its transformers. T_s and d denotes respectively the switching period and the controlled duty ratio. Figure 6 shows the operation converter. C_1, C_2, C_3 and C_4 denote, respectively, the control signals of the switches K_1, K_2, K_3 and K_4

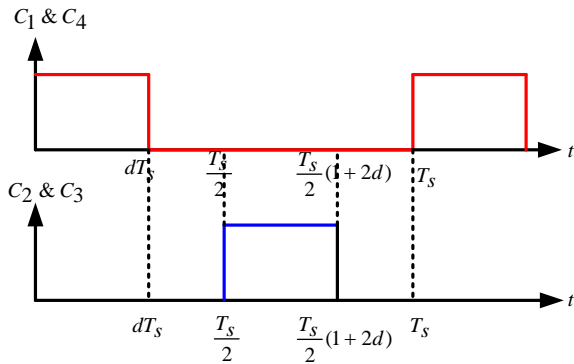


Figure 6: Key waveforms of the converter

There is two modes:

Mode 1: In this mode, the diagonally opposite switches (K_1 and K_4 or K_2 and K_3) are turned on during dT_s as shown in the following table. In this case fuel cell delivers the energy to load via resonant filter, two planar transformers and diodes.

Switches	$[0, dT_s]$	$[\frac{T_s}{2}, \frac{T_s}{2}(2d+1)]$
(K_1, K_4)	1	0
(K_2, K_3)	0	1

Mode 2: All switches are off and load current flow through diodes.

IX-AVERAGE MODEL OF DC-DC CONVERTER

For modeling the DC-DC converter, it is assumed:

- In the conducting state, each MOSFET is equivalent to a resistor r_t .
- In the conducting state, each diode is equivalent to a resistor.

r_d

- The charge and discharge of the capacitor C_r are instantaneous.
- The resistance of each non-conducting switch is infinite.
- The leakage inductance and the magnetizing of both transformers are neglected.

To model the converter we choose two state variables including capacitor voltage $V_0(t)$ and inductor current $i_L(t)$. The system state space representation is

$$\dot{x} = Ax + Bu \tag{6}$$

$$y = Cx + Du \tag{7}$$

Where u is the vector of inputs, y is the outputs and x is the status variables vector.

$$x = [i_L(t), v_0(t)]^T, u = V_{pac} \text{ and } y = v_0(t)$$

a) Mode 1

When the fuel cell has been started up, the system works in the stable operation mode as shows the table 1. In this case, the power flows from the fuel cell to the load through two diagonally transistors, resonant circuit, planar transformers and two diodes. The equivalent circuit is as follows

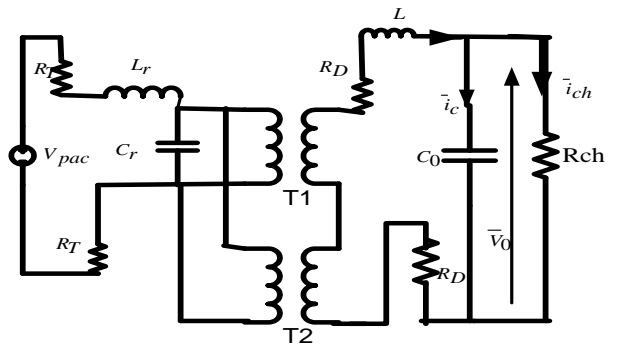


Figure 7: Equivalent circuit (mode 1)

If all impedance is transferred to the secondary winding, the equivalent circuit becomes the following

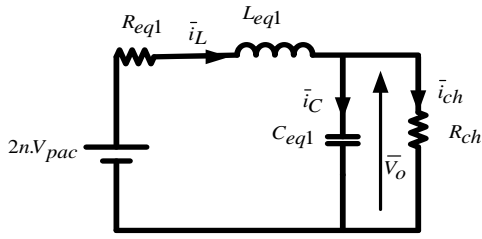


Figure 8: Referred secondary of the equivalent circuit

Where:

$$R_{eq1} = 2r_d + 2r_r * n^2 \quad (8)$$

$$L_{eq1} = L + n^2 L_r \quad (9)$$

$$C_{eq1} = C_0 + \frac{C_r}{n^2} \quad (10)$$

If we apply Kirchoff's law

$$\frac{di_L(t)}{dt} = -\frac{R_{eq1}}{L_{eq1}} i_L(t) - \frac{v_o(t)}{L_{eq1}} + \frac{2nV_{pac}}{L_{eq1}} \quad (11)$$

$$i_{Leq1}(t) = i_{Ceq1}(t) + i_{ch}(t) \quad (12)$$

$$\frac{dv_o(t)}{dt} = \frac{i_L(t)}{C_{eq1}} - \frac{v_o(t)}{R_{ch} * C_{eq1}} \quad (13)$$

$$\begin{pmatrix} \frac{di_L(t)}{dt} \\ \frac{dv_o(t)}{dt} \end{pmatrix} = \begin{pmatrix} -\frac{R_{eq1}}{L_{eq1}} & -\frac{1}{L_{eq1}} \\ \frac{1}{C_{eq1}} & -\frac{1}{R_{ch} * C_{eq1}} \end{pmatrix} \begin{pmatrix} i_L(t) \\ v_o(t) \end{pmatrix} + \begin{pmatrix} \frac{2n}{L_{eq1}} \\ 0 \end{pmatrix} V_{pac} \quad (14)$$

In the interval $[0, dT_s]$, the state space model and matrices are:

$$x' = A_1 x + B_1 u \text{ and } y = C_1 x$$

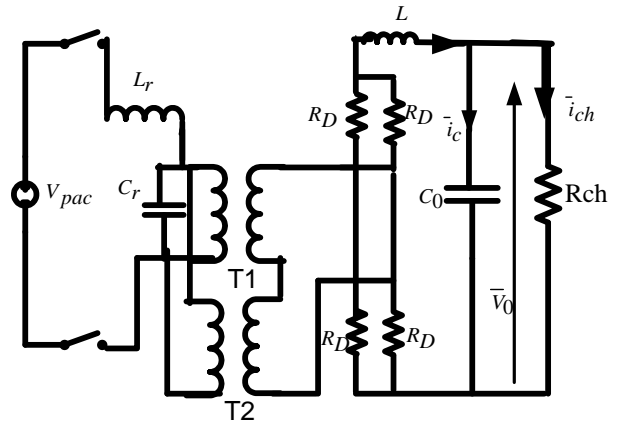
$$A_1 = \begin{pmatrix} \frac{-R_{eq1}}{L_{eq1}} & -\frac{1}{L_{eq1}} \\ \frac{1}{C_{eq1}} & -\frac{1}{R_{ch} * C_{eq1}} \end{pmatrix}$$

$$B_1 = \begin{pmatrix} \frac{2n}{L_{eq1}} \\ 0 \end{pmatrix}$$

$$C_1 = \begin{pmatrix} 0 \\ 1 \end{pmatrix}^T$$

b) Mode 2

The inductor current cannot equal to zero suddenly, so the two diodes are in conduction despite all switches are off. The equivalent circuit is show by figure 9



Figure

9: Equivalent circuit (Mode 2)

The equivalent circuit of the DC-DC converter referred to secondary winding is show in figure 10

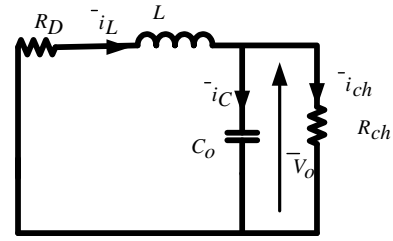


Figure 10: Referred secondary of the equivalent circuit(mode 2)

During the interval $[dT_s, T_s]$, the state space model and matrices are:

$$x' = A_2 x + B_2 u$$

$$y = C_2 x$$

Using Kirchoff law, we obtain :

$$\frac{di_L(t)}{dt} = -\frac{r_d}{L} i_L(t) - \frac{v_o(t)}{L} \quad (15)$$

$$\frac{dv_o(t)}{dt} = \frac{i_L(t)}{C_0} - \frac{v_o(t)}{R_{ch} * C_0} \quad (19)$$

$$A_2 = \begin{pmatrix} -\frac{r_d}{L} & -\frac{1}{L} \\ \frac{1}{C_0} & -\frac{1}{R_{ch} * C_0} \end{pmatrix} ; B_2 = \begin{pmatrix} 0 \\ 0 \end{pmatrix} \text{ and } C_2 = \begin{pmatrix} 0 \\ 1 \end{pmatrix}^T \quad (20)$$

The last half cycle is identical to the first half cycle, so during switching period, mode 1 and mode 2 are repeated twice. Finally, the averaged model state equation can be obtained

$$x' = A x + B u \quad (21)$$

$$y = C x$$

Where

$$A = A_1 2d + A_2 (1 - 2d)$$

$$= \begin{pmatrix} \frac{-2dR_{eq1}}{L_{eq1}} - (1-2d)\frac{r_d}{L} & -\frac{2d}{L_{eq1}} - \frac{(1-2d)}{L} \\ \frac{2d}{C_{eq1}} + \frac{(1-2d)}{C_0} & -\frac{2d}{R_{ch}C_{eq1}} - \frac{(1-2d)}{R_{ch}C_0} \end{pmatrix} \quad (22)$$

$$B = 2dB_1 + (1-2d)B_2 = \begin{pmatrix} \frac{4nd}{Leq} \\ 0 \end{pmatrix} \quad (23)$$

$$C = 2dC_1 + (1-2d)C_2 = \begin{pmatrix} 0 \\ 1 \end{pmatrix}^T \quad (24)$$

Average large signal circuit model is often derived as shown in figure 11.

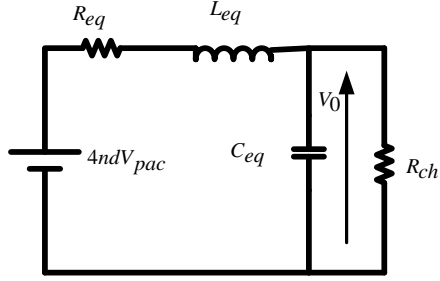


Figure 11: circuit model

Where

$$R_{eq} = 2d * R_1 + (1-2d)r_d(1 + \frac{n^2 L_r}{L}) \quad (25)$$

$$L_{eq} = \frac{L + n^2 L_r}{1 + n^2(1-2d)\frac{L_r}{L}} \quad (26)$$

$$C_{eq} = \frac{C_0 + \frac{C_r}{n^2}}{1 + (1-2d)\frac{C_r}{n^2 C_0}} \quad (27)$$

The elaborated model is simulated in Matab/Simulink with the following parameters:

Parameter	Value
Fuel Cell Voltage	$V_{pac} = 24V$
Switching Frequency	$f = 20Khz$
Resonant inductor	$L_r = 2\mu H$
Resonant capacitor	$C_r = 32\mu F$
Filter inductor	$L = 20mH$
Filter capacitor	$C_0 = 400\mu F$
Load resistance	$R_{ch} = 50\Omega$
Diode on resistor	$r_d = 0.006\Omega$
Mosfet on resistor	$r_l = 0.005\Omega$
Turn of transformer	$n_1 = 7$

In time 0.2s, the duty cycle change from 0.2 to 0.3. Figure 12 shows the simulation result.

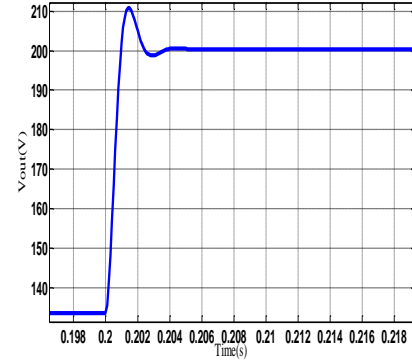


Figure 12: waveform of output voltage in changed duty Cycle

In time 0.4s, the resistor of load varies from 50Ω to 25Ω

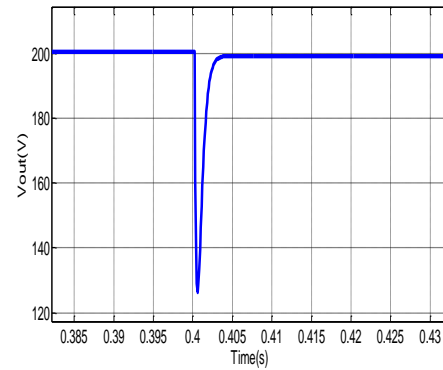


Figure 13: waveform of output voltage in changed load

V-SMALL SIGNALS ANALYSIS

The variables were analyzed to direct components (upper case letter) and a small ac perturbation (represented by($\tilde{\cdot}$))

$$x = X + \tilde{x}, d = D + \tilde{d}, v_0 = V_0 + \tilde{v}_0 \text{ and } v_{pac} = V_{pac} + \tilde{v}_{pac} \quad (28)$$

$$\tilde{x}' = x' \text{ because } X' = AX + BV_{pac} = 0 \quad (29)$$

$$X = -A^{-1}BV_{pac} \Rightarrow V_0 = -C.A^{-1}BV_{pac}$$

We can calculate the input to output transfer function

$$\frac{V_0}{V_{pac}} = \frac{4nDR_{ch}}{2D(R_{ch} + R_{eq}) + (1-2D)(R_{ch} + r_d)(1 + \frac{n^2}{L}L_r)} \quad (30)$$

The following figure shows the dc output to input gain versus duty cycle D . This figure proven that gain is linear versus the duty cycle.

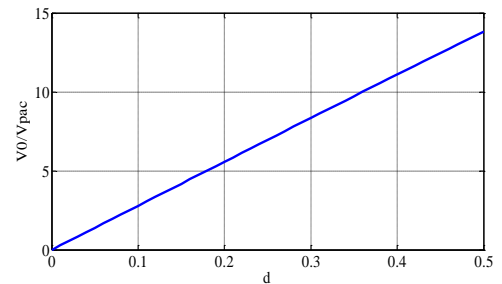


Figure 14: gain of converter versus duty cycle

when replacing each variable by its expression in (21) and using equation (29)

$$\begin{aligned} \tilde{x} &= A\tilde{x} + B\tilde{v}_{pac} + 2\tilde{d}((A_1 - A_2)X + (B_1 - B_2)V_{pac}) \\ &+ 2(A_1 - A_2)\tilde{d}\tilde{x} + 2(B_1 - B_2)\tilde{d}\tilde{x} \end{aligned} \quad (31)$$

Usually $2(A_1 - A_2)\tilde{d}\tilde{x} + 2(B_1 - B_2)\tilde{d}\tilde{v}_{pac}$ is negligible, so the equation (31) becomes

$$\tilde{x} = A\tilde{x} + B\tilde{v}_{pac} + 2\tilde{d}((A_1 - A_2)X + (B_1 - B_2)V_{pac}) \quad (32)$$

Using the Laplace transform:

$$\begin{aligned} \tilde{x}(s) &= (sI - A)^{-1} * ((A_1 - A_2)X + (B_1 - B_2)V_{pac}) + \\ &(sI - A)^{-1} B\tilde{v}_{pac} \end{aligned} \quad (33)$$

The expression of the output

$$\tilde{v}_0 = v_0 - V_0 = C(x - X) = (2(D + \tilde{d}) * C_1 + (1 - 2(D + \tilde{d}) * C_2)) * \tilde{x} \quad (34)$$

$$\text{If } 2(C_1 - C_2) * \tilde{d}\tilde{x} \text{ is negligible, } \tilde{v}_0 = C\tilde{x} + 2(C_1 - C_2)X\tilde{d} \quad (35)$$

Apply the Laplace transform to the equation(35) and using equation(33), we obtained

$$\begin{aligned} \tilde{v}_0(s) &= [C(sI - A)^{-1}((A_1 - A_2)X + (B_1 - B_2)V_{pac}) + \\ &(C_1 - C_2)X] 2\tilde{d}(s) + C(sI - A)^{-1} B\tilde{v}(s)_{pac} \end{aligned} \quad (36)$$

$H_1(s)$ and $H_2(s)$ denote respectively the transfer function from the output voltage to duty cycle and the transfer function from the output voltage to fuel cell voltage.

$$H_1(s) = \frac{\frac{2}{LC_0} (2nV_{pac} - I_L(r_d + 2n^2r_l))}{s^2 + s(\frac{R_2}{L} + \frac{1}{R_{ch}C_0}) + \frac{R_2}{R_{ch}C_0} + \frac{1}{LC_0}} \quad (37)$$

$$H_2(s) = \frac{\frac{4nD}{LC_0}}{s^2 + s(\frac{R_2}{L} + \frac{1}{R_{ch}C_0}) + \frac{R_2}{R_{ch}C_0} + \frac{1}{LC_0}} \quad (38)$$

Where $R_2 = r_d(1 + 2D) + 4Dn^2r_l$

A PID controller is used for regulating the output voltage of the converter DC-DC. The output voltage measured is compared with reference and compensates by changing in the duty cycle of switches as show the figure 14.

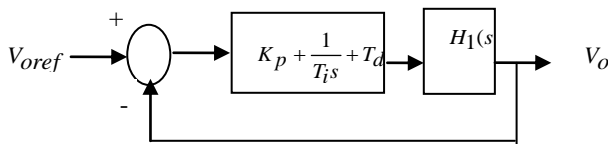


Figure 14: Closed loop control

Figure 15 shows the output voltage reference and the output voltage measured. It observed that for output voltage V_{oref} from 150V to 200V instantaneously, the output voltage V_o present a overtake equal to 5V.

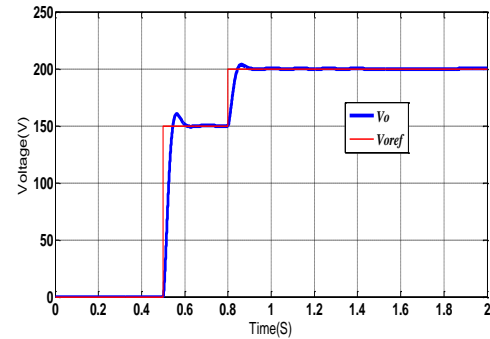


Figure 15: Small signal model for small various d

CONCLUSION

This paper has addressed the unidirectional DC-DC converter to be used in the fuel cell application in vehicle electrical .we have studied the average model of the converter .The developed model is verified in two cases (changed of duty cycle and load).and we are presented the small signal model and transfer functions from the output voltage to duty cycle and to fuel cell voltage .to improve the converter performance and stability , we chose the PID controller in the closed loop to adjust the output voltage in changing duty cycle.

REFERENCES

- [1] Y.Wu and H.W.Gao " optimization of fuel cell and super-capacitor for fuel cell electric vehicles ",IEEE Trans. Veh Technol.,vol 55 , n° 6,pp 1748-1755, Nov 2006.
- [2] E.Schaltz, A Khalig and P.O Rasmussen" Investigation of battery /ultra-capacitor energy storage rating for a fuel cell hybrid electric vehicle". IEEEVPPC.pp3882-3891.juin 2008.
- [3] M.Zandi,A.Paymen,J-P.Martin,S.Pierfederici,B.Davat and F.Tabar" Energy Management of a fuel Cell /super capacitor/ battery power source for electric vehicular applications" IEEE Trans.Veh Technol,vol 60 , n° 2,pp 433-443,February 2011.
- [4] S. Tsooulidis, E. Mitronikas, and A. Safacas " Comparative study of three types of step – up DC – DC Converters for Polymer Electrolyte Membrane Fuel Cell Applications" ISPEEDAM,pp 1303-1308,2010
- [5] R.Noroozian , M. Abedi, G. B. Gharehpetian and A. Bayat " On-grid and Off-grid Operation of Multi-Input Single-Output DC/DC Converter based Fuel Cell Generation System " Proceedings of ICEE . pp 735-758 , May 2010.
- [6] S. Chonsatidjamroen, KN. Areerak, and K L. Areerak " Dynamic Model of a Buck Converter with a Sliding Mode Control " WASET,pp 386-391,n°60; May 2011.
- [7] A.S. Samosir and A. H. M. Yatim" Dynamic Evolution Control of Bidirectional DC-DC Converter for Interfacing Ultra-capacitor Energy Storage to Fuel Cell Electric Vehicle System" ,AUPEC,pp 113-118,December 2008.
- [8] A.Ghadimi,H.Rastegar and A.Keyhani" development of average model for control of a fuel cell bridge PWM DC-DC converter " JIAEEE,vol 4,n°2,pp 52-59, March 2007.
- [9] X.Haiping ,W.Xuhui and K.Lu "Dual phase DC-DC converter in fuel cell electric vehicle " PECl,pp 92-97,October 2004.
- [10] G.Xie,X.Zhao,H.Fang and H.Xu" Averaged modeling of non ideal boost converter operating in discontinuous conduction mode " IJCEE, vol 3,n°1,pp 79-83, February 2011.

- [11] W.Na,B.Gou and T.Kim “Analysis and control of a bidirectional DC-DC converter for an ultra-capacitor in a fuel cell generation system” ,JEE: Theory and application, vol 1,pp 72-78, 2010.
- [12] Z.Zhang,R.Pittini,M.Andersen and O.Thomsen “A review and design of power electronics converters for fuel cell hybrid system applications” ELSEIVER,n° 20,pp 301-310, 2012.